

SUPPLEMENTARY MATERIAL

Physical properties of new ordered bimetallic phases  $M_{0.25}Cd_{0.75}PS_3$  ( $M = Zn^{II}$ ,  $Ni^{II}$ ,  $Co^{II}$ ,  $Mn^{II}$ ).

P. Fuentealba\*, C. Olea, H. Aguilar-Bolados, N. Audebrand, R. C. de Santana, C. Doerenkamp, H. Eckert, C. J. Magon, E. Spodine.

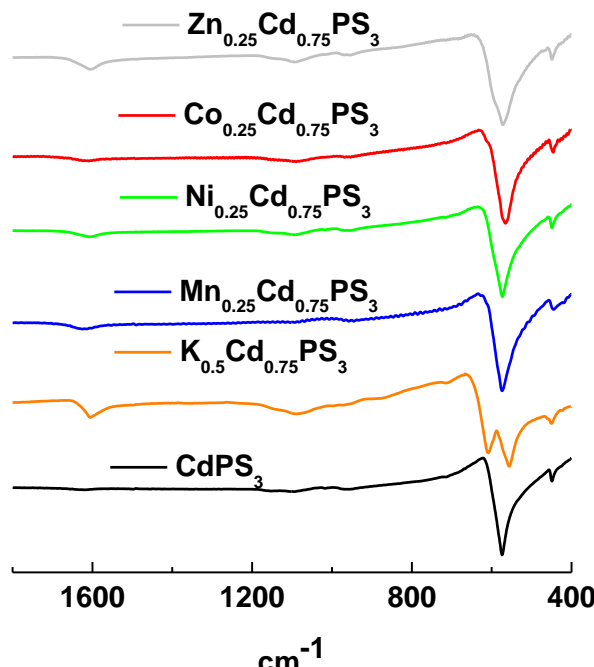


Fig. S1. FTIR

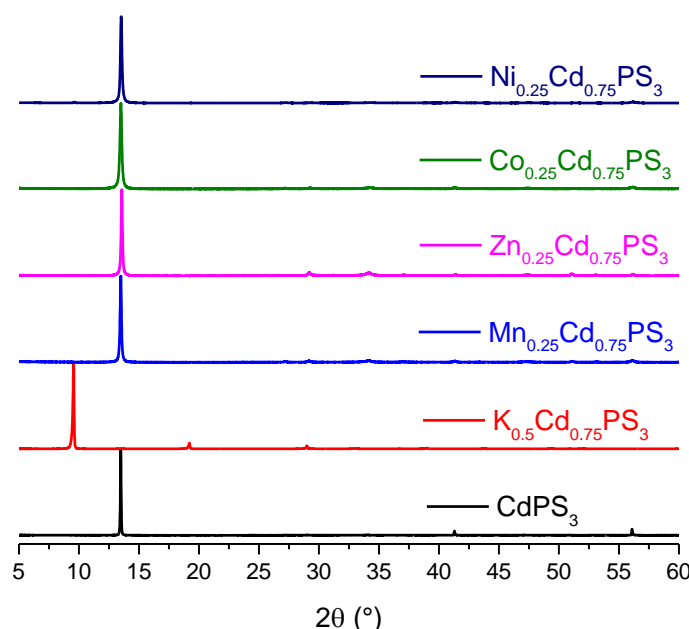


Fig. S2. Powder X-ray diffractograms of the lamellar phases.

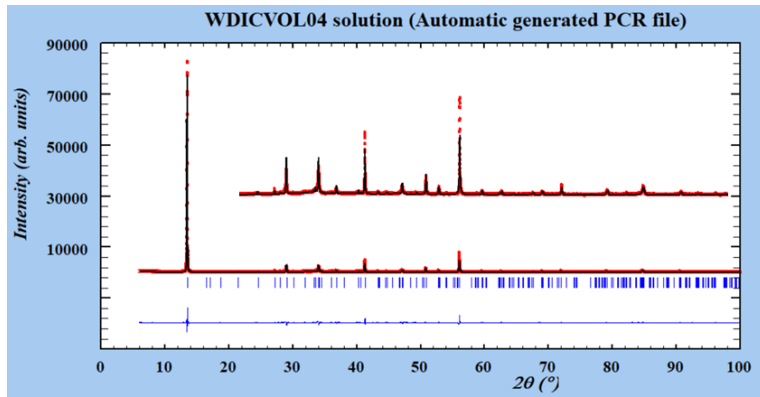


Fig. S2a: Refined powder X-ray diffractogram of  $\text{CdPS}_3$

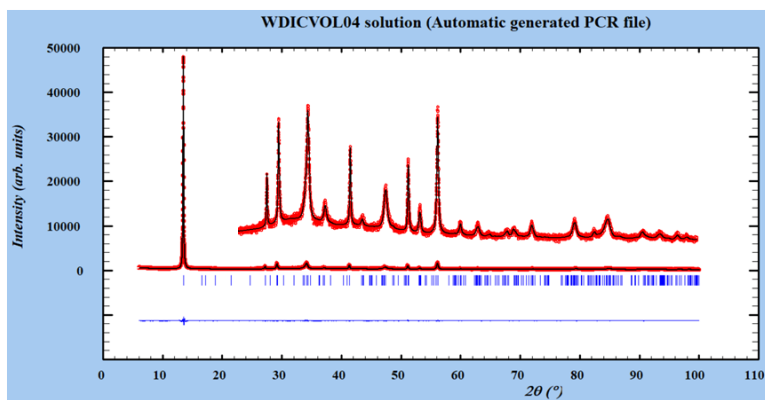


Fig. S2b: Refined powder X-ray diffractogram of  $\text{Mn}_{0.25}\text{Cd}_{0.75}\text{PS}_3$

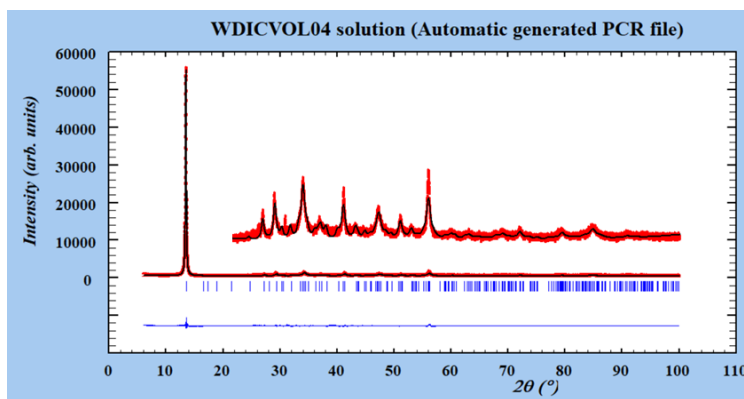


Fig. S2c: Refined powder X-ray diffractogram of  $\text{Co}_{0.25}\text{Cd}_{0.75}\text{PS}_3$ . Unknown small impurity line at 30.2.

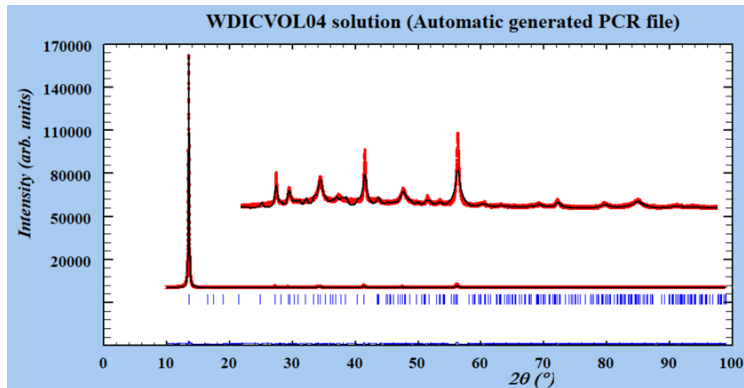


Fig. S2d: Refined powder X-ray diffractogram of  $\text{Ni}_{0.25}\text{Cd}_{0.75}\text{PS}_3$

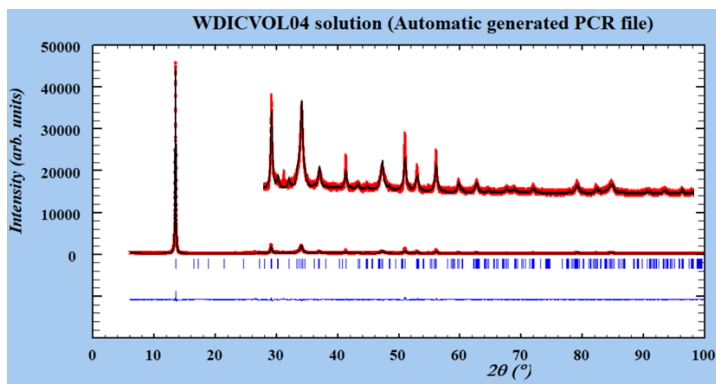


Fig. S2e: Refined powder X-ray diffractogram of  $\text{Zn}_{0.25}\text{Cd}_{0.75}\text{PS}_3$ . Unknown small impurity line at 30.2.

	$\text{CdPS}_3$	$\text{Mn}_{0.25}\text{Cd}_{0.75}\text{PS}_3$	$\text{Co}_{0.25}\text{Cd}_{0.75}\text{PS}_3$	$\text{Ni}_{0.25}\text{Cd}_{0.75}\text{PS}_3$	$\text{Zn}_{0.25}\text{Cd}_{0.75}\text{PS}_3$
$R_{\text{exp}}$	5.87	5.10	3.70	3.94	5.59
$\text{Chi}^2$	7.41	1.97	3.51	9.20	4.55
$R_p$	11.0	5.17	5.02	6.21	8.06
$R_{wp}$	16.0	7.17	6.93	11.9	11.9

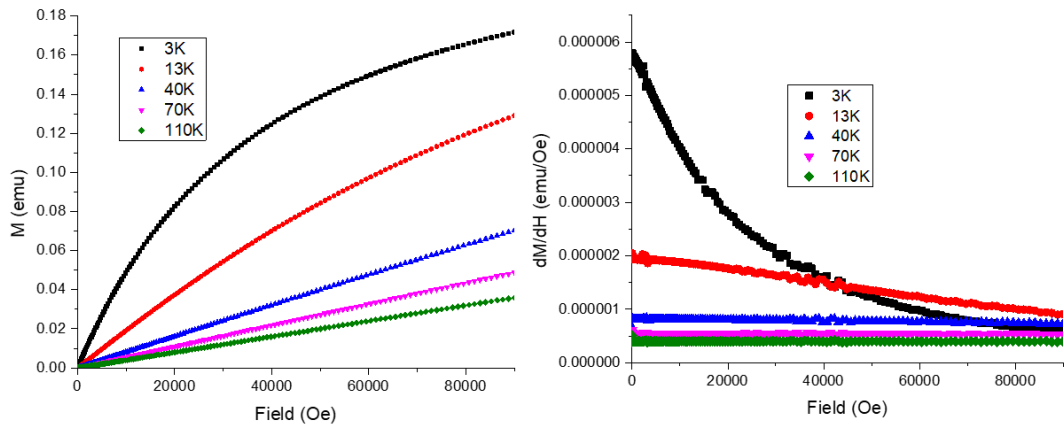


Fig. 3a.  $M(H)$  and first derivate curves for  $\text{Mn}_{0.25}\text{Cd}_{0.75}\text{PS}_3$ .

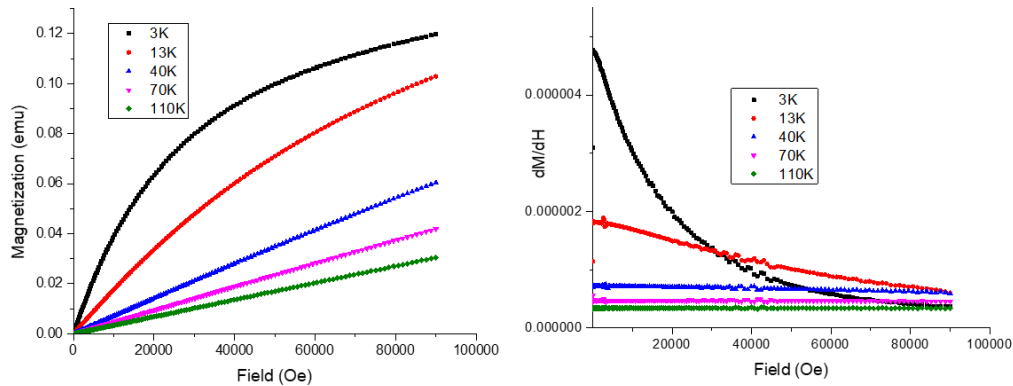


Fig S3b.  $M(H)$  and first derivate curves for  $\text{Co}_{0.25}\text{Cd}_{0.75}\text{PS}_3$ .

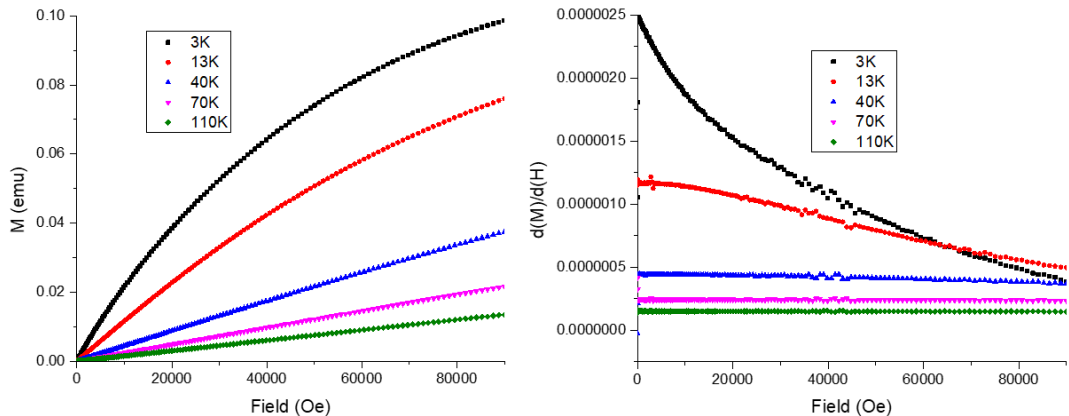


Fig. S3c.  $M(H)$  and first derivate curves for  $\text{Ni}_{0.25}\text{Cd}_{0.75}\text{PS}_3$ .

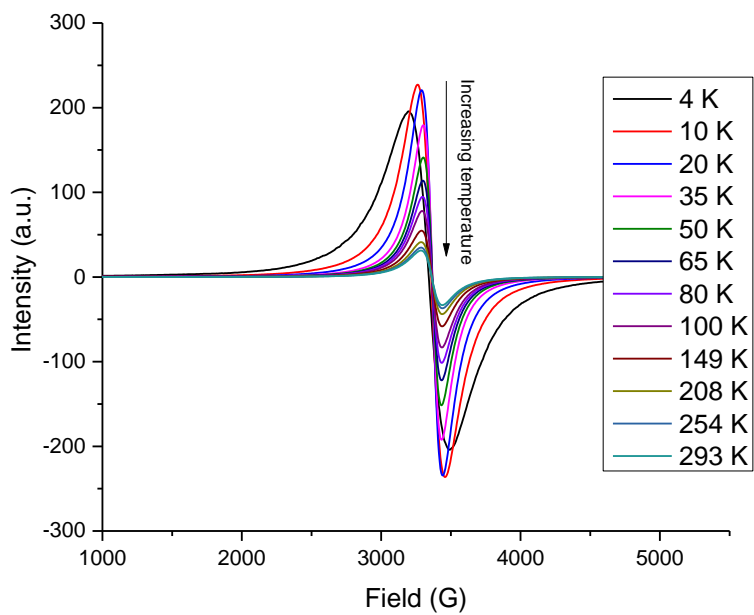


Fig. S4. EPR spectra of the  $\text{Mn}_{0.25}\text{Cd}_{0.75}\text{PS}_3$  phase.

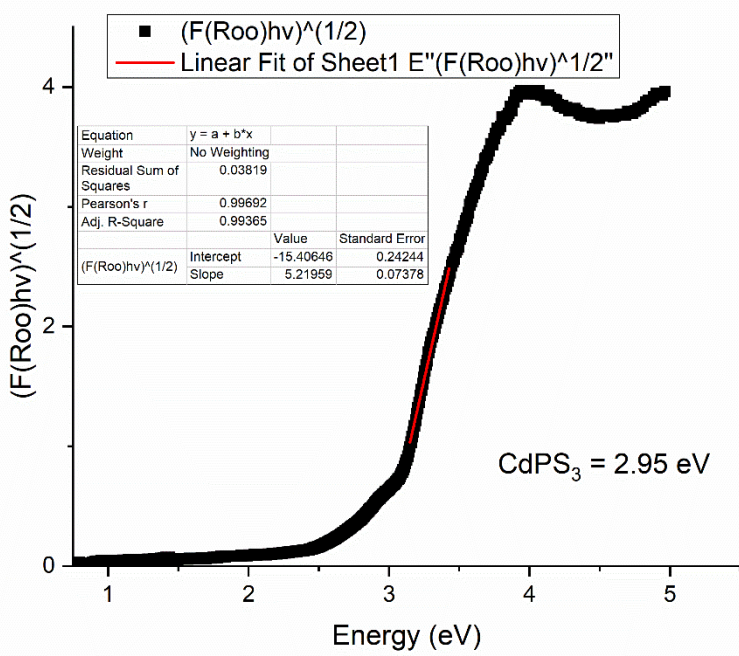


Fig. S5a Tauc plots for  $\text{CdPS}_3$

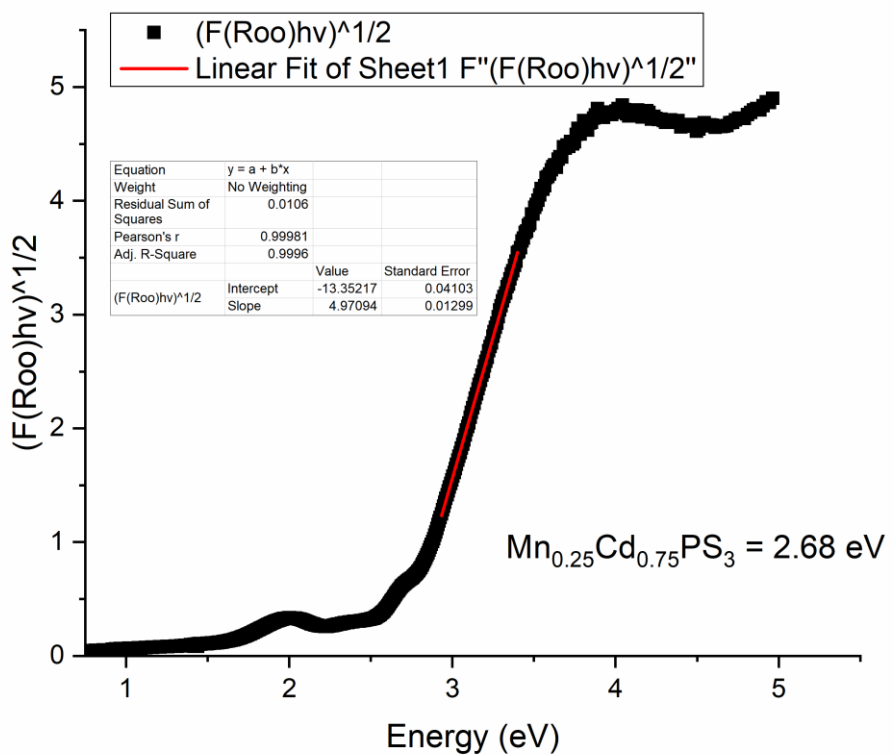


Fig. S5b Tauc plots for Mn<sub>0.25</sub>Cd<sub>0.75</sub>PS<sub>3</sub>

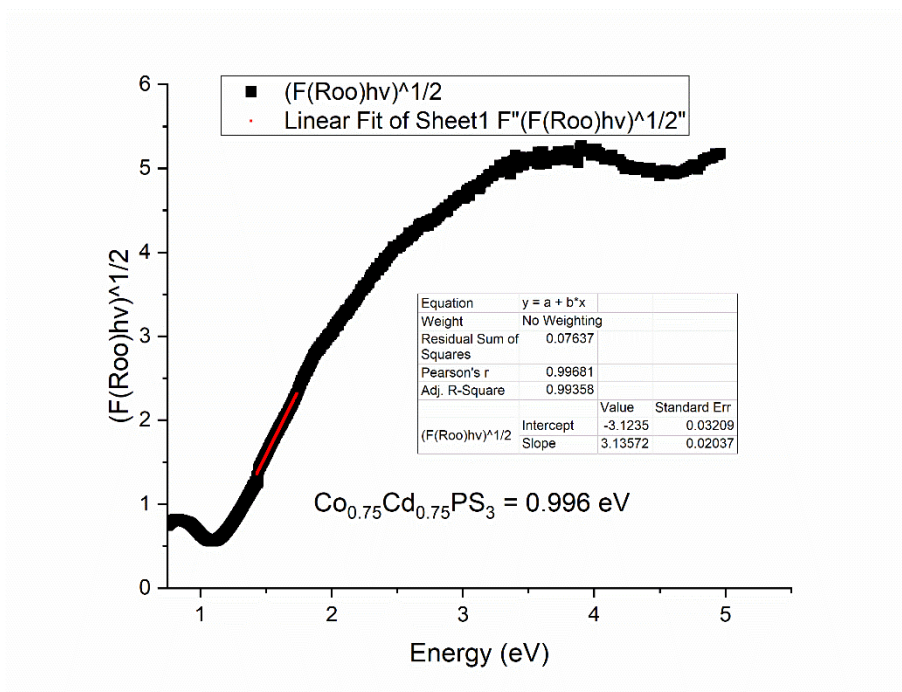


Fig. S5c Tauc plots for Co<sub>0.25</sub>Cd<sub>0.75</sub>PS<sub>3</sub>

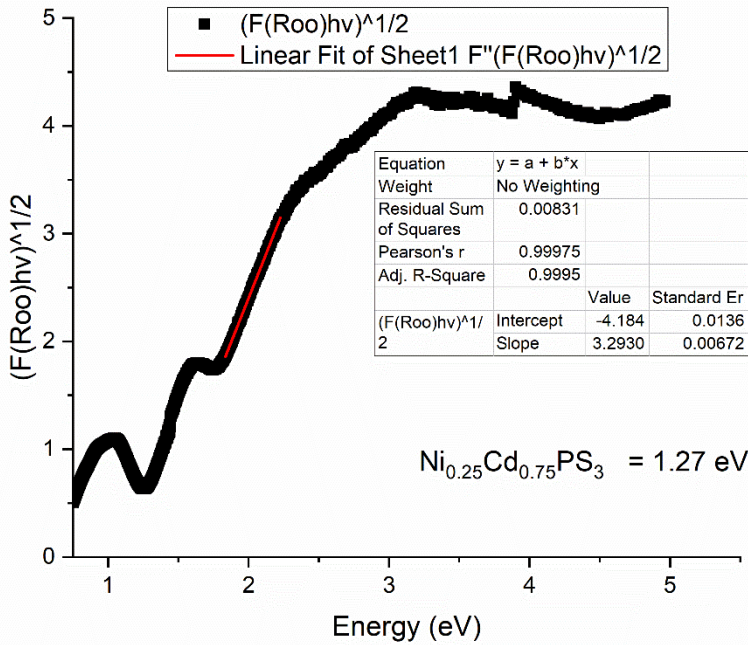


Fig. S5d Tauc plots for  $\text{Ni}_{0.25}\text{Cd}_{0.75}\text{PS}_3$

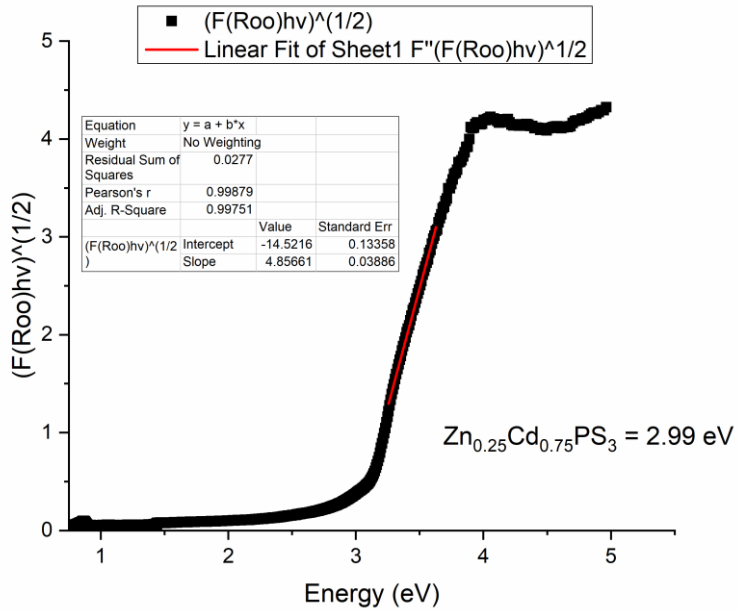


Fig. S5e Tauc plots for  $\text{Zn}_{0.25}\text{Cd}_{0.75}\text{PS}_3$

Table 1: Ionic radius <sup>1</sup>.

Element (six coordination sphere)	Ionic radii (pm)
Cd <sup>II</sup>	109
K <sup>I</sup>	138
Mn <sup>II</sup>	97
Co <sup>II</sup>	89
Ni <sup>II</sup>	83
Zn <sup>II</sup>	88

Equations for magnetic fittings:

$$\chi = \frac{C(x)}{T - \Theta(x)} \quad (1)$$

where the Curie constant, expressed in (emu K mol<sup>-1</sup>) is given by

$$C(x) = \frac{xN_A g^2 \mu_B^2 S(S+1)}{3k_B} \quad (2)$$

Table S2. The Rushbrook and Wood  $b_i$  coefficients calculated for honeycomb lattices with S = 5/2, 3/2 and 1, and x = 0.25.

S	$b_1$	$b_2$	$b_3$	$b_4$	$b_5$	$b_6$
5/2	-17.5	4.192	-8.720	-7.706	-30.723	-86.899
3/2	-1.875	2.111	-1.496	-0.375	1.835	0.008
1	-1	0.83	-0.511	-0.035	0.264	-0.201

### EPR Fittings

The spectrum was simulated by a sum of three components: an isotropic broad line and two axial sharper lines. S denote the spin value of each paramagnetic specie. The perpendicular and parallel values of the g-tensor are denoted by  $g_{\perp}$  and  $g_{\parallel}$ , respectively. Iwpp[G L] stands for the [Lorentzian Gaussian] line width for isotropic magnetic-field domain broadening (peak-to-peak, in Gauss). HStrain denote the Gaussian residual line width (full width at half height, in MHz), describing broadening due to unresolved hyperfine couplings. weight is a software parameter used to scale a multiple component spectrum. A linear baseline correction was used.

### References.

- 1 G. L. Miessler, P. J. Fischer and D. a Tarr, *Inorganic Chemistry*, Fifth Edit., 2013.